Biomedical Microdevices manuscript No.
(will be inserted by the editor)

Effect of Substrate Thermal Resistance on Space-Domain Microchannel Fluorescent Melting Curve Analysis

David J Kinahan[1], **Tara M Dalton**[1,2], **Mark RD Davies**[1,2]

[1] Stokes Bio Ltd

Henry St

Limerick

Ireland

[2] Stokes Institute

Department of Mechanical and Aeronautical Engineering

University of Limerick

Ireland

Received: date / Revised version: date

Abstract In recent years, Fluorescent Melting Curve Analysis (FMCA) has become an almost ubiquitous feature of commercial quantitative PCR (qPCR) thermal cyclers. Here a micro-fluidic device is presented capable of performing FMCA within a microchannel. The device consists of modular thermally conductive blocks which can sandwich a microfluidic substrate. Opposing ends of the blocks are held at differing temperatures and a linear thermal gradient is generated along the microfluidic channel. Fluorescent measurements taken from a sample as it passes along the micro-fluidic channel permits fluorescent melting curves to be generated. In this study we measure DNA melting temperature from two plasmid fragments. The effects of flow velocity and ramp-rate are investigated, and measured melting curves are compared to those acquired from a commercially available PCR thermocycler.

1 Introduction

Fluorescent Melting Curve Analysis (FMCA) is a technique through which non-specific fluorescent DNA dyes can be used to recognise an individual DNA product (Wittwer & Kusukawa, 2004). The thermodynamic stability of double strand DNA (dsDNA) is dependant on both its length and its base pair composition (Wittwer

et al., 1997a; Ririe et al., 1997); and so samples of differing length and compositions may be recognised by their differing denaturation temperatures, t_m. FMCA uses the characteristic variations in sample fluorescence with temperature to identify the denaturation temperature of samples. With increasing temperature, the fluorescence of dsDNA in the presence of a dsDNA dye will decrease linearly. However at higher temperatures — typically between $85°C$ and $95°C$ — the dsDNA denatures and a rapid, non-linear decrease in fluorescence will be observed. The measurement of the temperature at which this non-linear change in fluorescence occurs permits measurement of the denaturation temperature of PCR product.

FMCA has become an almost ubiquitous feature of quantitative PCR thermocyclers (Herrmann et al., 2006); and is most commonly used as a closed tube technique to ensure the specificity and quality of the PCR sample amplified. However, the melting curve method can be used to detect single nucleotide polymorphisms (SNPs) (Gundry et al., 2003) and mutations associated with genetic diseases such as cancer (Bernard & Wittwer, 2002). When combined with appropriate primer/probe selection melting curve analysis becomes an important tool in multiplex PCR (Hernandez et al., 2003). Melting analysis has been performed on volumes as low as $10nl$ using a custom microfluidic platform (Sundberg et al., 2007).

Since the Micro Total Analysis System (μTAS) concept was first proposed (Manz et al., 1990), a number of technologies have undergone miniaturisation from desktop to 'lab on a chip'. Among these technologies have been the thermocyclers associated with the PCR process. Well-based PCR thermocyclers aimed at μTAS applications have focused on reducing reaction size (Nagai et al., 2001). Space-domain (flowing) PCR, where the reaction is moved between zones of fixed temperature (Kopp et al., 1998; Schneegass & Kohler, 2001) has been of interest to many research groups due to its potential for rapid thermocycling, small reaction volumes and high-throughput processing.

Progress towards developing FMCA for use with flowing thermocyclers is ongoing. The application of a linear temperature gradient across a micro-fluidic substrate has previously been applied to micro-channel based systems (Mao et al., 2002; Dalton et al., 2005; Crews et al., 2008; Kinahan et al., 2008a) for DNA melting analysis. Denaturation temperature measurements made from surface bound DNA have previously been used to characterise microfluidic substrates (Dodge et al., 2004).

In this paper, melting curve analysis is performed by pumping DNA in solution along a microfluidic channel. The test platform consists of two thermal blocks which sandwich a microfluidic channel. This fluidic channel is transparent, Teflon FEP tubing with an internal diameter of $400\mu m$. In the course of experimental testing, the channel is aligned within the test platform using a substrate composed of polycarbonate. DNA melting curves are measured in each substrate at a variety of

different flow velocities and ramp-rates. Melting curves acquired from the platform are compared with those acquired from commercially available PCR thermocyclers.

2 Biological Material

Two individual PCR fragments were amplified from E. Coli plasmid vector pGEM-5Zf(+) (Promega). Two primer pairs were used. A 240bp sample was amplified using a forward primer of sequence 5'- AGG GTT TTC CCA GTC ACG ACG TT-3' and a reverse primer 5'-CAG GAA ACA GCT ATG ACC-3'. A 232bp fragment, was amplified using forward primer 5'-ATA CCT GTC CGC CTT TCT CC-3' and reverse primer 5'-CCT CGC TCT GCT AAT CCT GT-3'. Primers were acquired from MWG Biotech (Ebersberg, Germany). Samples were amplified using LightCycler Faststart DNA Master SYBR Green I reaction mix (Roche). Samples were thermocycled and a melting curve analysis performed using the Applied Biosystems AB7900 thermocycler. Samples were then frozen at $-20°C$ before use. Melting curves for samples acquired using the ABI7900 thermocycler may be seen in Figure 5.

3 Experiment Design and Methods

The sample carrying channel used during experimentation is a transparent, disposable Teflon FEP tubing (Upchurch Scientific) with an outer diameter of approximately $800\mu m$ and inner diameter of approximately $400\mu m$.

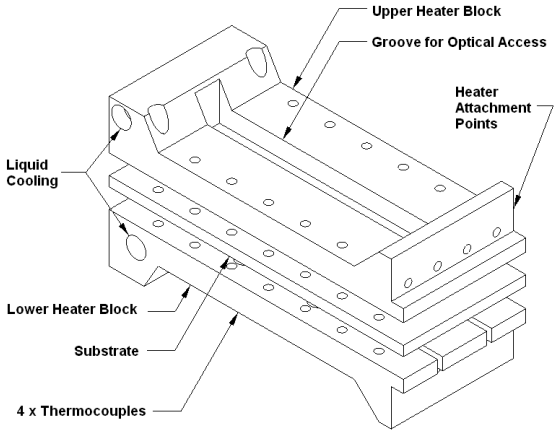

Fig. 1 Exploded view of heater block configuration.

The test device consists of two aluminium blocks of length 120mm, width 50mm and minimum thickness 10mm, as shown in Fig 1, which are designed to sandwich the sample carrying channel. The channel is aligned with the thermal blocks using a substrate, which is manufactured from polycarbonate. The polycarbonate substrate has a groove machined into which the sample carrying channel fits. The substrate is then covered with a transparent polycarbonate sheet. One end of the thermal blocks have thick film heaters and Darlington transistors attached for heating, while the opposite end of the blocks have channels machined facilitate liquid cooling via a precision thermal bath. As illustrated in Figure 1, a slot of dimensions 84mm long and 2mm wide is machined into the upper block to provide optical access to the substrate. Four thermocouples are embedded in the lower thermal block such that they align with the optical access groove when the blocks are mated.

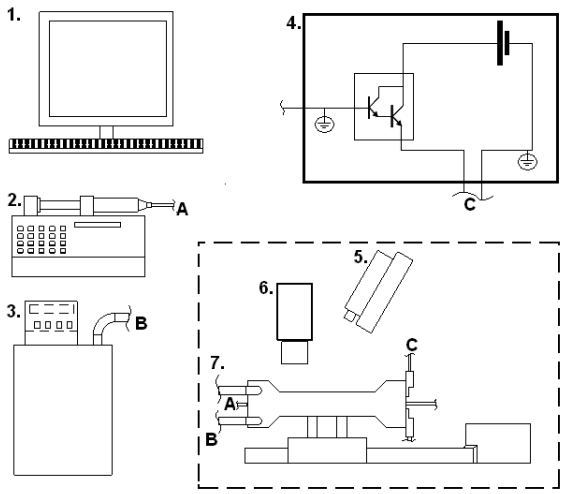

Fig. 2 Schematic of Equipment Setup. 1. Computer for control/datalogging. 2. Syringe Pump. 3. Heater bath for cooling. 4. Control circuit for heaters. 5. Excitation Laser. 6. Monochrome Camera. 7. Rig mounted on Positioning Stage. A-A, B-B and C-C indicate connections for wiring and tubing.

Samples are loaded into the Teflon FEP tubing via aspiration, and are buffered by an immiscible fluid (M5904 Mineral Oil - Sigma-Aldrich). Samples are slugs approximately 100mm long ($12.5\mu l$), which is greater than the interrogation length (length of optical window) of the device. As the recirculation length for the sample (Kashid et al., 2005) is significantly greater than the interrogation length it is assumed that multiphasic effects are trivial and the flow is assumed to approximate single phase Hagen-Poissuele flow. The sample is then pumped into the device until it is observed entering the interrogation area, and a fluorescent signal is acquired.

Fluorescent illumination was provided using a 488nm blue laser (BlueSkyResearch). The laser beam was passed through a concave lens (Edmundoptics) to expand and diffuse the excitation beam. Emissions were filtered via a 515nm long pass filter (Melles-Griot) and the emission sensor was a monochrome CCD camera (The Imaging Source). Fluorescent emissions are proportional to the intensity of excitation light (Haugland, 2002). Therefore, in order to ensure uniform illumination of the interrogation area throughout individual experiments, the heating blocks are mounted on a positioning stage. As the sample flows down the capillary at a given velocity, the test device is moved at a velocity of identical magnitude but in the opposite direction, so the sample remains within the interrogation area, and stationary relative to the excitation light source and emission sensor. Sample pumping is via a syringe pump (Harvard Apparatus PHD2000). The experimental setup is illustrated in Figure 2.

Upon starting each experiment, the appropriate flow rate for the syringe pump is automatically calculated based on the user-selected ramp rate. The traverse velocity of the positioning stage is similarly calculated. The experimental conditions at which testing took place is outlined in Table 1. In some cases the sample was aspirated back through the device and then re-tested.

In order to identify the actual denaturation temperature, t_m, for each sample an analysis method was applied to the melting curves generated. Due to the inaccuracies present in the melting peak method of detecting DNA melting temperatures, particularly for noisy data, a method based on the technique outlined by Gundry

Table 1 Experimental Test Conditions.

Ramp Rate	Temp. Diff	Thermal Grad	Velocity
$^\circ C/s$	$^\circ C$	$^\circ C/mm$	mm/s
0.000	24	0.286	0.000
0.033	24	0.286	0.116
0.033	8	0.095	0.350
0.100	24	0.286	0.350
0.100	8	0.095	1.050
0.300	24	0.286	1.050
0.300	8	0.095	3.150

et al. (2003) was applied. Gundry et al. (2003) states that the denaturation temperature of each sample is the temperature at which half the DNA strands present have denatured. Therefore the denaturation temperature is that temperature at which the fluorescence of the sample is half way between that of a wholly double stranded DNA and that of fully denatured DNA.

The sample melting curve data is smoothed using Savitsky-Golay moving average smoothing (Savitzky & Golay, 1964) with a smoothing interval of $1^\circ C$ and is then normalised between 0 and 1. A line of best fit is fitted to the linear fluorescent data, which occurs before the sample melting transition. This section of the melting curve is selected manually. Minimal fluorescence was detected post melting transition in every case, and hence it is assumed that a line of best fit through this data would coincide with the x-axis of the melting plot. Through the intersection of the line of best fit with the x-axis a line of half the slope of the original line is drawn. The intersection of this line with the melting curve indicates the point at which half the DNA strands present have been denatured, as can be seen in Figure 3.

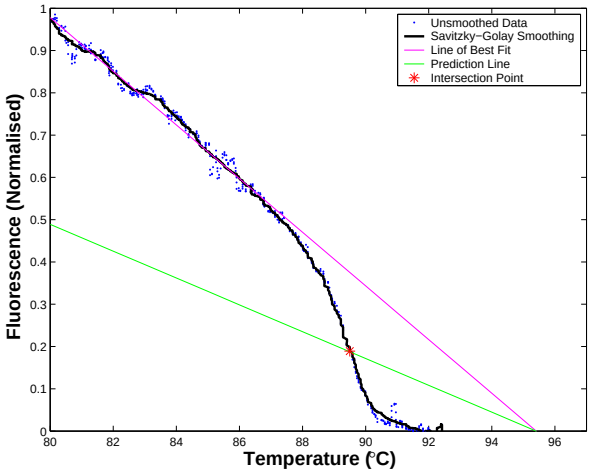

Fig. 3 Demonstration of the method used to determine the denaturation temperature, t_m, of a sample from its melting curve. Plasmid A, the 240bp sample, measured at $\frac{dT}{dt} = 0.10^\circ C/s$ and $\Delta T = 24^\circ C$.

4 Heat Transfer

A feature of flowing PCR thermocylers is rapid transition of fluid temperature between thermal zones. Beyond short entry lengths, the fluid within the thermal zones is isothermal. However, in the case of melting analysis, it is advantageous that the fluid be subject to constant heating. Therefore, the thermal resistance of both the fluid and the tubing walls will result in a temperature variation ΔT between the fluid temperature and the temperature at the outer substrate walls. The temperature variation is proportional to the ramp-rate seen by the

fluid $\frac{dT}{dt}$, which is in turn a product of the fluid velocity, v, and the spatial thermal gradient applied across the blocks $\frac{dT}{dx}$. The temperature variation is also proportional to the thermal resistance of the fluid and the tubing walls.

Equation 1 describes the temperature variation expected across the walls of a cylindrical tube ΔT_T, where δy is an integral length along the direction of fluid flow, x_T is the thickness of the tubing, k_T the thermal conductivity of the tubing, R the inner radius of the tubing, c_w the thermal capacitance of the working fluid and ρ_w the density of the working fluid.

$$\Delta T_T = -\left(\frac{dT}{dt}\right)\left(\frac{x_T}{k_T\left(2\pi R\delta y\right)}\right)\left(c_w\rho_w\pi R^2\delta y\right) \quad (1)$$

Based on Bejan (1993), Equation 2 presents the temperature variation across the fluid within the microchannel, $\Delta T(r)$,

$$\Delta T(r) = -\frac{dT}{dt}\left(1 + 0.5(1 - \frac{r^2}{R^2})\right)\frac{\left(R^2 - r^2\right)}{4\alpha_w} \quad (2)$$

where r the position on the radial axis measured from the centre-line, R the radius of the circular microchannel and α the thermal diffusivity of the working fluid $\frac{kw}{\rho_w c_w}$.

Equations 1 and 2 are more fully described in Kinahan et al. (2008b) and are supported using numerical simulation. In microchannel-based melting analysis Equations 1 and 2 describe a temperature offset which is proportional to ramp-rate, and which must be compensated for when making comparisons between different platforms. Similar effects were identified for well based melting platforms by Ririe et al. (1997).

5 Results

The 240bp and 232bp DNA samples were tested under the operating conditions described in Table 1. For cases of $\frac{dT}{dt} = 0°C$ the sample was positioned within the experimental platforms so that the long plug of fluid filled most of the optical access window. With the fluid held stationary, the optical detection system traverses the rig at a velocity equivalent to that used to measure samples at $\frac{dT}{dt} = 0.1°C/s$. For the dataset presented in Figure 4, the sample did not fully fill the optical window, which results in the increase in fluorescence seen at $72°C$ in Figure 4(a) where the fluid being measured changes from mineral oil to PCR solution.

For measurements at $\frac{dT}{dt} = 0.0°C/s$ and $\frac{dT}{dt} = 0.1°C/s$ typically ≈ 900 fluorescent measurements are made during the traverse of the sample across the optical access window. For the case of $\frac{dT}{dt} = 0.033°C/s \approx 2700$ measurements are made; for $\frac{dT}{dt} = 0.3°C/s \approx 300$ measurements are made and for $\frac{dT}{dt} = 0.9°C/s \approx 100$ measurements are made. For experiments conducted with a temperature difference of $\Delta T = 8.0°C$ across the optical access groove the number of measurements are typically reduced by a factor of 3 as these tests occur at higher velocities.

Figure 4 presents a dataset acquired for the 240bp sample. In this case, a single sample was tested and recycled through the experimental rig for re-testing under different test conditions. It is clear from this dataset that melting curves measured using the platform for the same test conditions are highly repeatable, with a maximum $0.3°C$ variation of $t_m s$ measured for a particular test condition. However, also of note is the effect recycling the sample had upon the melting profiles measured. The first test of this particular sample occurred at $\frac{dT}{dt} = 0.1°C/s$ and is shown in Figure 4(c). For subsequent tests at these conditions the melting profile shows a fluorescent decrease at $\approx 80°C$.

The recycling procedure involved aspirating the sample back through the experimental test rig. The 'backward' motion of the slug through the test rig results in it being subjected to slow, steady cooling. A primary cause of primer dimer and other non-specific amplification during the PCR process is the use of long dwell times at the denaturation and annealing stages of the PCR process (Wittwer et al., 1997b); while conversely rapid-cycling between PCR thermal zones results in increased PCR efficiency and specificity. Although a fully amplified sample, it may be inferred that the repeated slow heating and cooling of the PCR sample promotes the generation of primer dimer from the excess primers contained within the solution.

It is assumed that the melting profile change at $\approx 80°C$ is a result of primer-dimer. In some later tests using this sample, such as that shown in Figure 4(b), a slight increase in fluorescence is observed prior to final sample denaturation. Zhou et al. (2004) states that SYBR Green I, the dye used during the course of these experiments, preferentially binds to shorter dipolymers in preference to longer fragments. Hence, it is inferred that these melting profiles show a redistribution of SYBR Green I dye from the denatured primer-dimers to the target strand. Of note it is clear from Figure 4(c) that the presence of excess primer-dimer within the sample does not have an observable effect upon the measured denaturation temperature. In addition, this feature was not observed in melting curves generated for the 232bp sample, possibly due to the use of lower concentrations of primers within the assay.

Figure 4(e) shows one melting curve from each of the ramp rates applied to the sample using a spatial temperature gradient of $\Delta T = 24°C$. It is clear that varying the ramp-rate (velocity) of the fluid has an observable effect upon the melting profiles acquired; and the denaturation temperatures measured. This effect is similarly shown in Figure 4(f) for a spatial temperature gradient of $\Delta T = 8°C$. Figures 5(a) and 5(b) demonstrate this effect with greater clarity. In Figure 5(a), melting curves acquired at near identical velocities but different ramp-rates — due to different spatial temperature gradients — are compared, and show a large difference in measured denaturation temperature. However, Figure 5(b) shows two samples measured at different velocitiexs and differ-

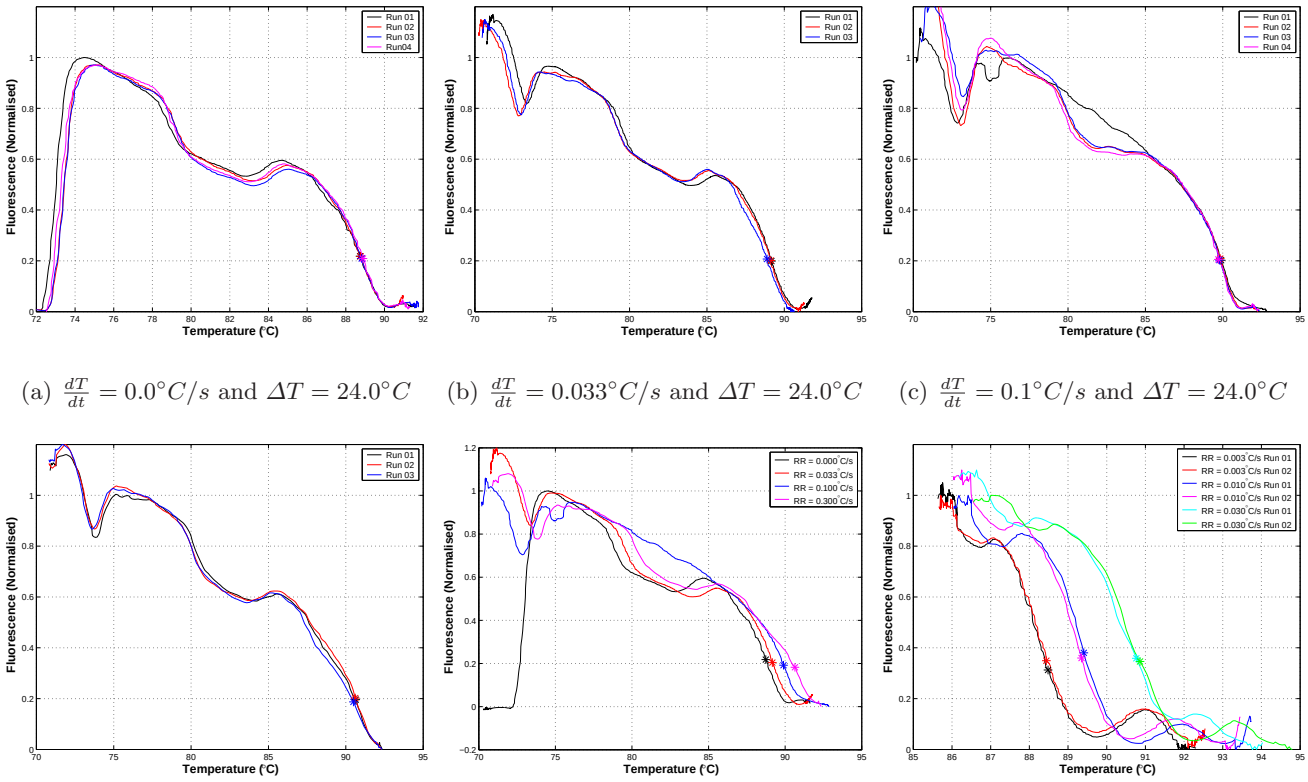

(a) $\frac{dT}{dt} = 0.0°C/s$ and $\Delta T = 24.0°C$ (b) $\frac{dT}{dt} = 0.033°C/s$ and $\Delta T = 24.0°C$ (c) $\frac{dT}{dt} = 0.1°C/s$ and $\Delta T = 24.0°C$

(d) $\frac{dT}{dt} = 0.3°C/s$ and $\Delta T = 24.0°C$ (e) Different Ramp Rates and $\Delta T = 24.0°C$ (f) Different Ramp Rates and $\Delta T = 8.0°C$

Fig. 4 Sample A (240bp) Melting Curves measured at various velocities and ramp-rates. A typical melting curve acquired for this sample using a commercial PCR platform may be seen in Figure 5(c).

ent spatial temperature gradients, but identical ramp-rates. In this case the measured denaturation temperatures correspond closely.

Figure 5(c) shows two melting curves measured for different samples — 240bp and 232bp plasmid fragments — using identical test conditions. Comparison with similar samples measured using a commercial thermocycler — particularly when offset in the temperature axis as shown in Figure 5(d) — show that the microchannel melting curve method can be used to discern between two samples. In these plots, raw unsmoothed data is presented. Approximately 900 data acquisitions are made using the space-domain melting analysis method, compared to approximately 80 for the commercial PCR thermocycler. The noisier signal from the space-domain method is most likely caused by variations in the optical quality of the microchannel.

6 Discussion and Conclusion

The ability of microchannel melting analysis to differentiate between DNA amplicons of different melting temperature has been demonstrated. The accuracy and re-

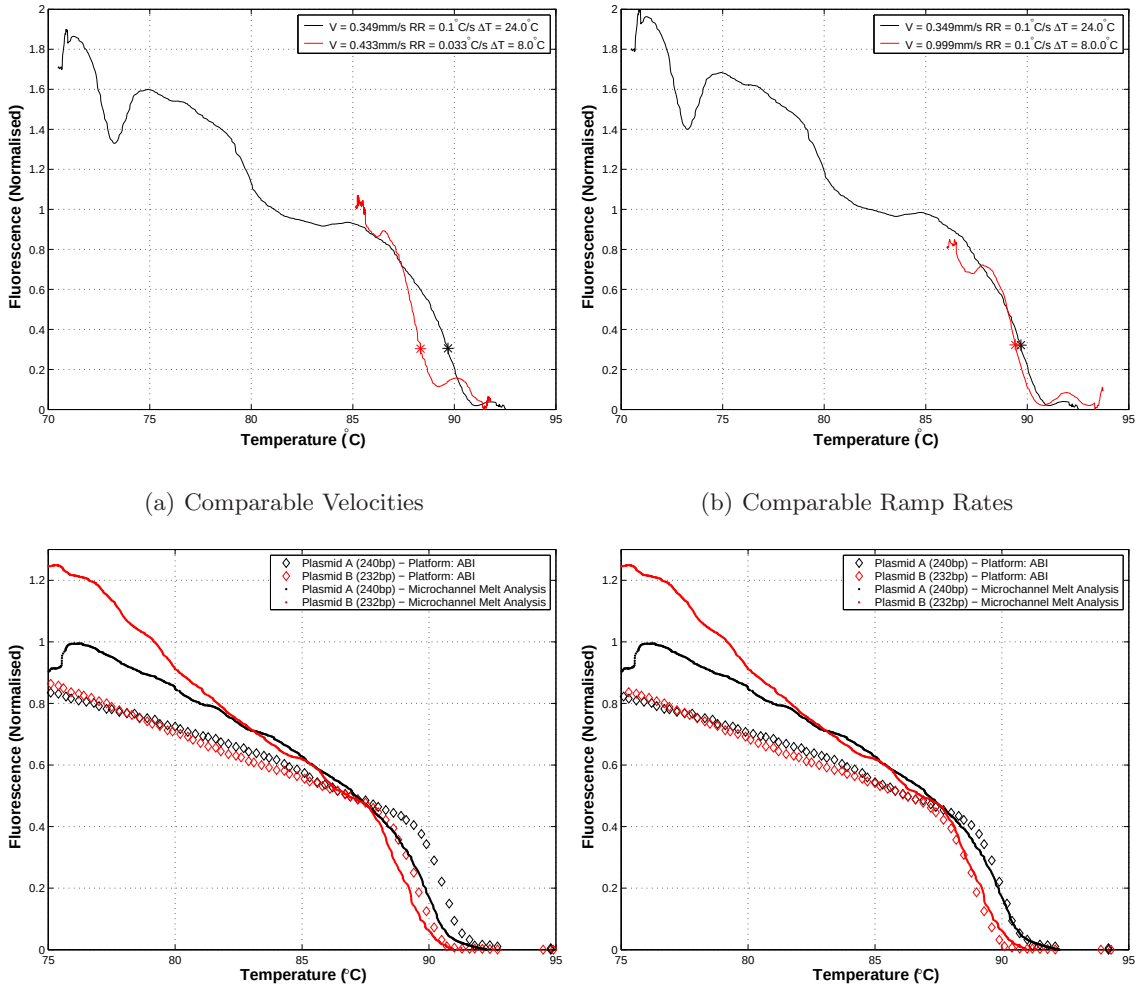

(a) Comparable Velocities

(b) Comparable Ramp Rates

(c) Measured Temperatures

(d) Offset Temperatures

Fig. 5 Comparison of melting curves acquired for Plasmid Fragment A(240bp). Melting curves are generated at either comparable velocities or comparable ramp-rates. Differentiation of Plasmid DNA samples using the experimental test rig. Comparison of Plasmid Fragment A(240bp) DNA strand melting curves with Plasmid Fragment B(232bp) melting curves. Melting curves are acquired at a ramp rate of $\frac{dT}{dt} = 0.1°C/s$ with a temperature difference of $\Delta T = 24.0°C$ applied across the optical access groove. Comparison is made to melting curves acquired using the ABI Prism® 7900HT commercial thermocycler. Figure 5(d) offsets the commercial melting curves by $-0.6°C$.

peatability of the denaturation temperatures measured under individual test conditions demonstrate the potential for an approach such as this to be applied to a μTAS system at the output of a flowing PCR thermocycler.

Thick walled, low conductivity plastic tubing has been used with success in flowing PCR thermocyclers (Sayers et al., 2006; Chabert et al., 2006). With PCR the flow transitions between 2 or 3 isothermal zones. Hence, past the entry length, the heat flux required to maintain fluid

temperature is minimal. Therefore the temperature distribution through thick walled tubing is minimal; the fluid and tubing walls may be considered isothermal. Giordano et al. (2001) describes how a primary advantage of using glass as a working material for μTAS applications is its low thermal conductivity. However in the case of microchannel melting analysis a constant heat flux is required to heat the fluid throughout the analysis. Therefore the tubing walls/glass substrates act as an insulating layer between the heater blocks and the sample, resulting in a temperature disparity between the outer walls of the substrate and the actual fluid temperature.

The magnitude of this temperature disparity is proportional to the thermal resistance between the fluid and the heater blocks and to the ramp-rate seen by the fluid. The ramp-rate is a product of the spatial temperature gradient and the velocity of the fluid flow. It is clear from the results presented here that the temperature disparity is observable and will have an effect on denaturation temperature measurements. An equation has been presented which predicts the temperature disparity for fluid in a simple tube. Kinahan et al. (2008b) has described how this approach can be applied to any micro-channel substrate to compensate for temperature disparity effects irrespective of knowledge of substrate dimensions or composition; with the caveats that the spatial temperature gradient applied to the walls of the substrate be uniform, and the substrate be non-varying in the direction of heat flux.

However, it has also been shown that measurements made at different velocities/spatial temperature gradients but at identical ramp-rates are comparable. This approach has a number of advantages. In the case of an integrated μTAS system where flow rates are dictated by other factors, changing the spatial temperature gradient applied along the block allows the ramp-rate to be selected. Decreasing the velocity of the fluid — and hence the time the sample is in the test rig — can result in a greater number of fluorescent $acq/^{\circ}C$ being made. The number of fluorescent $acq/^{\circ}C$ made by a high-resolution melting analysis platform is an important benchmark for its performance, particularly in SNP analysis (Herrmann et al., 2006). Melting curves measured at $\frac{dT}{dt} = 0.033^{\circ}C$ across $\Delta T = 24^{\circ}C$ resulted in approximately $100 acq/^{\circ}C$.

Of particular note were measurements made at $\frac{dT}{dt} = 0.0^{\circ}C$. In this case, the velocity of the fluid was zero, and the fluorescent acquisition system was traversed across the sample. Using this method, it is clear that no ramp-rate effects occur. Indeed, unlike well-based systems (Ririe et al., 1997) this approach will not require any compensation for thermal capacitance effects. In addition, the number of fluorescent measurements made will be entirely a function of the viability of the test sample, resulting in the potential for very high resolution analysis.

As fluorimeters were integrated into traditional PCR thermocyclers and made quantitative PCR (qPCR) possible, it is clear that the next step in the development

of flowing PCR thermocyclers on the micro-scale will be the integration of some manner of fluorescent detection (Sayers et al., 2006; Chabert et al., 2006). Well-based melting curve analysis offers a simple, closed tube addition to the well-based PCR thermocycler for applications in quality control, multiplexing and SNP detection; similarly microchannel melting analysis has the potential to be integrated into flowing PCR thermocycler systems and can offer much the same functionality.

References

A. Bejan (1993). *Heat Transfer*. John Wiley and Sons.

P. Bernard & C. Wittwer (2002). 'Real Time PCR Technology for Cancer Diagnostics'. *Clinical Chemistry* **48**:1178–1185.

M. Chabert, et al. (2006). 'Automated Microdroplet Platform for Sample Manipulation and Polymerase Chain Reaction'. *Anal Chem* **78**:7722–7728.

N. Crews, et al. (2008). 'Product Differentiation during continuous-flow thermal gradient PCR'. *Lab on a Chip* **8**:919–924.

T. M. Dalton, et al. (2005). 'Fluorescent Melting Curve Analysis compatible with a Flowing Polymerase Chain Reactor'. In *Proceedings of 2005 ASME International Mechanical Engineering Congress and Exposition*. ASME.

A. Dodge, et al. (2004). 'A Microfluidic Platform Using Molecular Beacon-Based Temperature Calibration for Thermal Dehybridization of Surface-Bound DNA'. *Analytical Chemistry* **76**(6):1778–1787.

B. Giordano, et al. (2001). 'Towards dynamic coating of glass microchip chambers for amplifying DNA via the polymerase chain reaction'. *Electrophoresis* **22**(2):334–340.

C. Gundry, et al. (2003). 'Amplicon Melting Analysis with Labled Primers: A Closed-Tube Method for Differentiating Homozygotes and Heterozygotes'. *Clinical Chemistry* **49**(3):396–406.

P. Haugland (2002). *Handbook of Flourescent Probes and Research Products*. Molecular Probes, Oregon.

M. Hernandez, et al. (2003). 'Development of melting temperature based SYBR Green I polymerase chain reaction methods for multiplex genetically modified organism detection'. *Analytical Biochemistry* **323**:164–170.

M. G. Herrmann, et al. (2006). 'Amplicon DNA Melting Analysis for Mutation Scanning and Genotyping: Cross-Platform Comparison of Instruments and Dyes'. *Clinical Chemistry* **52**(3):494–503.

M. N. Kashid, et al. (2005). 'Internal Circulation with the Liquid Slugs of a Liquid-Liquid Slug-Flow Capillary Microreactor'. *Ind. Eng. Chem. Res* **44**:5003–5010.

D. J. Kinahan, et al. (2008a). 'ICNMM2008-62014 Microchannel Fluorescent Melting Curve Analysis'. In *Proceedings of 2008 Sixth International Conference on Nanochannels, Microchannels and Minichannels*.

ASME.

D. J. Kinahan, et al. (2008b). 'ICNMM2008-62015 Thermal Resistance Measurements from a Microchannel Fluorescent Melting Curve Analysis Platform'. In *Proceedings of the 2008 6th International Conference on Nanchannels, Microchannels and Minichannels*. ASME.

M. Kopp, et al. (1998). 'Chemical Amplification: Continuous-Flow PCR on a Chip'. *Science* **280**:1046–1048.

A. Manz, et al. (1990). 'Miniaturized total chemical analysis systems: A novel concept for chemical sensing'. *Sensors and Actuators B: Chemical* **1**:244–248.

H. Mao, et al. (2002). 'Reusable Platforms for High-Throughput On-Chip Temperature Gradient Assays'. *Analytical Chemistry* **71**:5071–5075.

H. Nagai, et al. (2001). 'Development of A Microchamer Array for Picoliter PCR'. *Analytical Chemistry* **73**:1043–1047.

K. Ririe, et al. (1997). 'Product Differentiation by Analysis of DNA Melting Curves during the Polymerase Chain Reaction'. *Analytical Biochemistry* **245**:154–160.

A. Savitzky & M. J. E. Golay (1964). 'Smoothing and Differentiation of Data by Simplified Least Squares Procedures'. *Analytical Chemistry* **36**:1627–1639.

M. B. Sayers, et al. (2006). 'Real-Time Fluorescence Monitoring of the Polymerase Chain Reaction in a Novel Continuous Flow Reactor for Accurate DNA Quantification'. In *Proceedings of 4th International Conference on Nanochannels, Microchannels and Minichannels*. ASME.

I. Schneegass & J. Kohler (2001). 'Flow-through polymerase chain reactions in chip thermocyclers'. *Reviews in Molecular Biotechnology* **82**:101–121.

S. O. Sundberg, et al. (2007). 'Solution-phase DNA mutation scanning and SNP genotyping by nanoliter melting analysis'. *Biomedical Microdevices* **9**(2):159–166.

C. Wittwer, et al. (1997a). 'Continuous fluorescence monitoring of rapid cycle DNA amplification'. *Biotechniques* **22**:130–138.

C. Wittwer & N. Kusukawa (2004). *Molecular Microbiology: Diagnostic Principles and Practice*, chap. 6 Real Time PCR. ASM Press, Washington DC.

C. Wittwer, et al. (1997b). 'The LightCycler: a microvolume multisample fluorimeter with rapid temperature control'. *Biotechniques* **22**:176–181.

L. Zhou, et al. (2004). 'Closed-tube genotyping with unlabeled oligonucleotide probes and a saturating DNA dye'. *Clinical Chemistry* **50**(8):1328–1335.